ELSEVIER

Polymer 44 (2003) 2249–2254

polymer

www.elsevier.com/locate/polymer

The synthesis and morphology characteristic study of BAO-ODPA polyimide/TiO_2 nano hybrid films

Pei-Chun Chiang, Wha-Tzong Whang*

Department of Materials Science and Engineering, National Chiao Tung University, HsinChu 300, Taiwan, ROC

Received 19 September 2002; accepted 16 January 2003

Abstract

Hybrid nanocomposite films of titanium dioxide (TiO_2) in polyimide (PI) from 2,5-bis(4-aminophenyl)-1,3,4-oxadiazole (BAO) and 4,4′-oxydiphthalic anhydride (ODPA) have been successfully fabricated by an in situ sol–gel process. These nanocomposite films exhibit fair good optical transparency up to 40 wt% of TiO_2 content. X-ray diffraction spectroscopy shows three sharp peaks in pure BAO-ODPA PI. It results from the intermolecular regularity. However, the intermolecular regularity in the hybrid film is disrupted by the introduction of TiO_2 nanoparticles with no sharp peak in XRD spectra. Fourier transform infrared (FTIR) and X-ray photoelectron spectroscopy (XPS) results confirm the formation of TiO_2 particles in PI matrix. The surface Ti content is much lower than the theoretical bulk content in all hybrid films. The ratio of the former to the latter increases with the TiO_2 content and levels off at TiO_2 wt% $\geq$ 20. Transmission electron microscope (TEM) images show that the TiO_2 phase is well dispersed in the polymer matrix. The size of the TiO_2 phase increases from 10 to 40 nm when the TiO_2 content is 5–30 wt%, respectively.

Keywords: Polyimide; Nanostructured TiO_2; Sol–gel process

1. Introduction

A wide range of polymer and inorganic have been combined to form nanocomposite materials with unique mechanical, electrical, magnetic and adhesive properties [1–6]. This is related to some distinctive properties of nanoparticles and anomalous cooperative properties of systems. Applications of hybrid materials in gas separation and optoelectronic devices have been extensively reported, such as high-refractive-index, waveguide materials, anti-refractive coating and optical devices [19,36–38]. Polyimide (PI) has been the topic of intensive studies due to its outstanding electrical, mechanical and thermal properties [7–9]. Therefore, PI is a promising candidate type for the matrix of these hybrids. Metal-containing PI were first reported by Angelo [10], who added organometallic complexes to several types of PI and described the metallic contents, dielectric constants and volume resistivity for the copper-containing PI. PI films containing metal/metal oxide particles have been widely reported in the literature [11–15], but the studies of polyimide–titanium dioxide (PI/TiO_2) nanocomposite materials are limited. PI/TiO_2 hybrid materials prepared from various poly(amic acid) (PAA) precursors and coupling agents have been studied [16–18]. However, increasing the content of titanium oxide causes the films opaque and the agglomeration of the titanium oxide into large particles.

In this study, we make an attempt to investigate the optical properties of metal-containing polyimides as thermally stable polymeric materials that have some interesting optical functions in the visible region. Besides, we develop an in situ formation of nanosized titanium oxide by using acetylacetone (acac) as a chelating agent to stabilize the titanium alkoxide. No extra acid catalyst and water are added to the PAA solution, and the amount of acac is adjusted to avoid gelation. The main reason is that acac can reduce the reaction rate through the formation of an acetylacetate complex [17,20]. Furthermore, nanosized metal particles are known to have interesting optical properties. Prior to describing the specific applications to optical communication use, we report here the thermogravimetric analysis (TGA), X-ray diffraction spectroscopy (XRD), X-ray photoelectron spectroscopy (XPS), transmission

* Corresponding author. Tel.: +886-3573-1873; fax: +886-3572-4727.
E-mail address: wtwhang@msn.com (W.T. Whang).

0032-3861/03/$ - see front matter © 2003 Elsevier Science Ltd. All rights reserved.
doi:10.1016/S0032-3861(03)00086-7

electron microscope (TEM), and basic optical properties of metal-containing hybrid films.

2. Experimental section

2.1. Materials

2,5-Bis(4-aminophenyl)-1,3,4-oxadiazole (BAO) obtained from Fluka was vacuum-dried for 3 h at 110 °C prior to use. 4,4′-Oxydiphthalic anhydride (ODPA) from TCI was purified by recrystallization from a high-purity acetic anhydride and then dried in a vacuum oven at 120 °C for at least 14 h. Tetraethyl orthotitanate ($Ti(OEt)_4$) and acetylacetone (acac) were available from TCI and Fluka, respectively. *N*,*N*-Dimethylformamide (DMF) from TCI was dried over molecular sieves.

2.2. Preparation of the PI/TiO_2 hybrid films

The synthesis of the PI/TiO_2 hybrid films was carried out according to the Fig. 1. In a 100 ml, three-necked round-bottomed flask fitted with a mechanical stirrer, a nitrogen inlet tube and a gas outlet tube 2.52 g (0.01 mol) of BAO was dissolved in 31.8 g of DMF. Dried ODPA powder 3.1 g (0.01 mol) was then added into the solution by five portions at 15% solids content (w/w). It is better to ensure the complete dissolution of the prior portion before adding a fresh portion. After the dissolution of all ODPA, the poly(amic acid) (PAA) mixture was further stirred for 2 h at ambient temperature. The desired amounts of $Ti(OEt)_4$ and acac were completely mixed and added dropwise into the poly(amic acid) (PAA) with vigorously stirring to avoid local inhomogeneities. The mixing was proceeded with continuous stirring for another 12 h. The theoretically calculated content of TiO_2 in the hybrid films is 5, 10, 15, 20, 30, 40 wt%. The weight percent was calculated under an assumption that all the $Ti(OEt)_4$ and PAA precursors converted to TiO_2 and PI after baking. The molar ratio of $Ti(OEt)_4$ to acac was fixed to 1:4. The mixture precursors were coated on the PET film using a doctor blade. The films were first soft-backed at 70 °C for 10 min in an air-circulating oven, then transferred to a rectangle stainless frame clamps and heated at the curing steps 100 °C (1 h), 150 °C (1 h), 200 °C (1 h) and 300 °C (10 h).

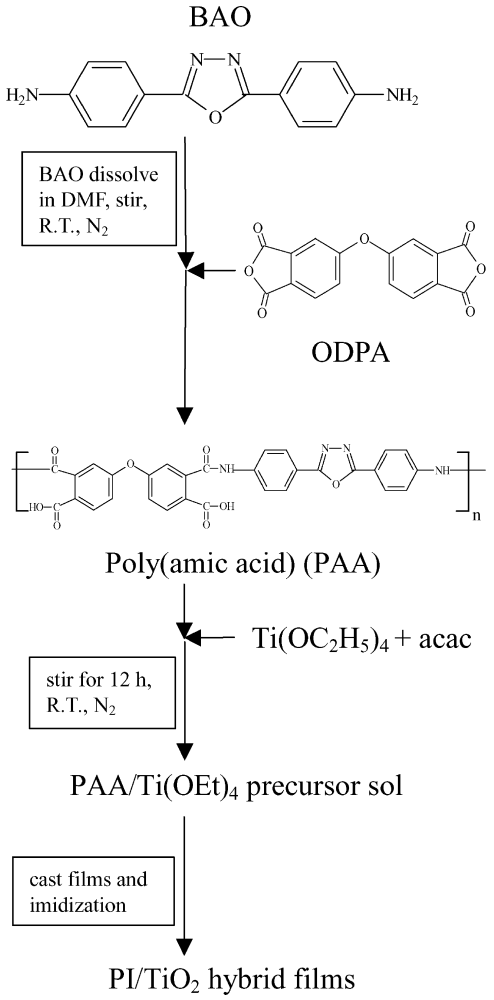

Fig. 1. Flow chart of the procedures to prepare the PI/TiO_2 hybrid films.

2.3. Measurements

FTIR absorption spectra were recorded between 4000 and 400 cm^{-1} by Nicolet PROTÉGÉ-460. UV–visible absorbance spectra were collected on an Agilent 8453 spectrometer. Samples were spin-coated on quartz glass and heated. X-ray diffraction analysis was done by using a MacScience MXP model X-ray diffractometer. The equipment was operated with Cu Kα radiation, operating at 50 kV, 100 mA, and a scanning speed of 4 degree min^{-1} at steps of 0.02°. XPS spectra were obtained by using a ESCA PHI 1600 spectrometer working in the constant analyzer energy mode with a pass energy of 50 eV and Mg Kα (1253.6 eV) radiation as the excitation source. XPS analysis was done at room temperature and pressures below 10^{-10} Torr. The take-off angle used in the XPS measurements was 90°. TEM was performed by employing a JEOL-200 FX transmission electron microscope. The samples for TEM study were first prepared by putting PI/TiO_2 hybrid films into epoxy capsules and curing the epoxy at 70 °C for 24 h in vacuum. The samples were then microtomed with Leica Ultracut Uct into 90 nm thick slices on which 3 nm thick carbon layer was deposited after the slices were moved to a TEM copper grid. Thermal analyses of the PI/TiO_2 hybrid films were performed by a TA TGA 2950. The measurements were carried out under nitrogen with a heating rate of 20 °C/min from 30 to 800 °C. The polymer decomposition temperature (Td) was determined at the temperature of 5% weight loss.

3. Results and discussion

The chemical structures of PI and PI/TiO_2 nanocomposite films are characterized with a FTIR spectroscopy as shown in Fig. 2. The characteristic peaks of symmetric C=O stretching and asymmetric C=O stretching of the imide group are clearly visible at ~1720 and ~1780 cm^{-1}, respectively. The assignment of the stretching of the imide ring is at 1380 cm^{-1} [21]. The mentioned peaks are the characteristic absorption of imide group and have been shown in the spectra of the entire PI film and PI/TiO_2 hybrid films. Besides, the introduction of the TiO_2 leads to a broad and strong absorption band in the range of 400 to 850 cm^{-1} [22,23]. Accordingly, as shown in Fig. 2 the intensity of this region rises with increasing TiO_2 content. The band at 3400–3500 cm^{-1} is a result of the Ti–OH group [24]. The bands near 1623 and 1105 cm^{-1} are assigned to the Ti–O and Ti–O–C stretching modes [25]. However, the above absorption bands are not clear when the TiO_2 content is small.

UV–visible spectra of the hybrid films with different TiO_2 content are shown in Fig. 3. Absorbance band is observed below 400 nm for pure PI. The spectrum of PI/TiO_2-5 wt% hybrid film is almost the same as pure PI. When the content of TiO_2 is equal to or more than 10 wt%, a relatively stronger absorbance can be seen at $\lambda \geq 450$ nm wavelength. Based on the UV–visible results, the low TiO_2 content is expected to produce more transparent films than those prepared from higher TiO_2 content. The raise in absorbance with the increase of TiO_2 content may be resulted from a complex formed during preparation of the precursor [20]. As we know, acac is a rather strong chelating ligand. The enolic form of β-diketones contains a reactive hydroxy group that reacts readily with metal alkoxides. Therefore, acac has often been reported in the sol–gel literature as a stabilizing agent for metal alkoxide precursors

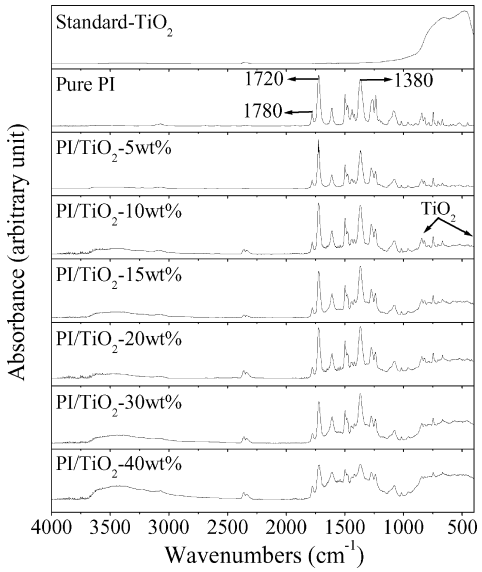

Fig. 2. FTIR absorption spectra of the PI/TiO_2 hybrid films.

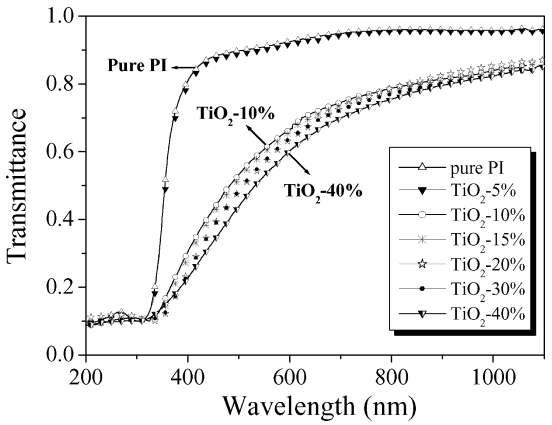

Fig. 3. UV-visible spectra of the PI/TiO_2 hybrid films.

[39]. Another interesting observation from Fig. 3 is the drastically increase of the absorbance curve between 5 and 10 wt%. This result may be attributed to the aggregation of metal oxide thereby causing growth of particle size and hence lead to large scattering [18]. However, the particle size of metal oxide is still in the nano scale.

XRD patterns for the pure PI, hybrid films and standard TiO_2 (anatase) powder are given in Fig. 4. Both pure PI and standard TiO_2 (anatase) powder show crystalline structures. The main diffraction peaks for pure PI are found at $2\theta = 15.7$, 22.1 and 24.8° corresponding to d-spaces of 5.65, 4.01 and 3.58 Å, respectively. It may be due to the intermolecular structure because the crystalline structure disappears after hybridizing TiO_2 nanostructure in the PI film. Some, not many, crystalline PI structure are reported [26–30]. The XRD patterns of the hybrid films display only a very broad

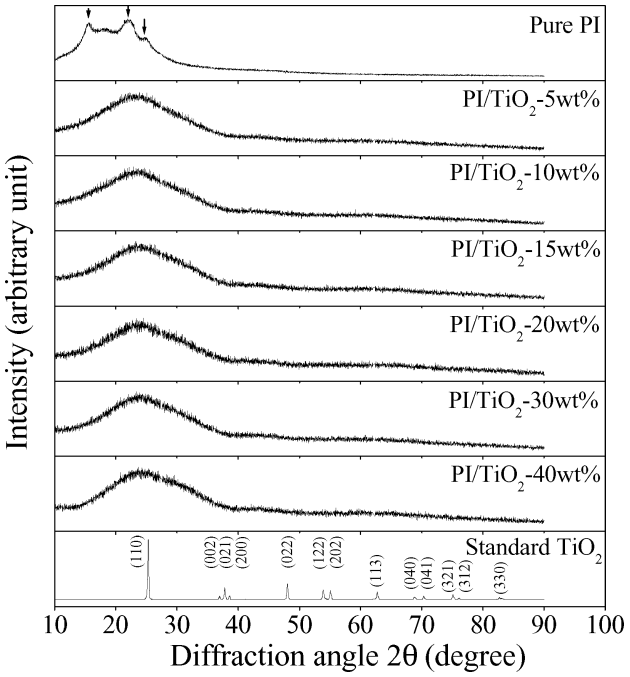

Fig. 4. X-ray diffraction spectra of pure PI, hybrid films and standard TiO_2 (anatae).

hump centered at $2\theta = 24°$, originating from amorphous phase of aromatic polyimide. This result indicates that TiO_2 do not form sufficiently large clusters for XRD during imidization [11]. Thus, the introduction of TiO_2 disrupts the PI intermolecular regularity.

Figs. 5–7 show further characterization of titanium species presented in polyimide matrices by XPS. Fig. 5 indicates the presence of carbon, oxygen, nitrogen and titanium. Figs. 6 and 7 give the binding energies of Ti 2p photoelectron peaks at 458.5 and 464.4 eV for Ti $2p_{3/2}$ and Ti $2p_{1/2}$ lines, respectively [17,31–33]. Besides, the XPS spectra of PI/TiO_2-30 wt% hybrid film sputtered at different times were recorded in Fig. 6. It is obvious that longer sputtering times result in an increase in the concentration of the titanium species.That implies there is a smaller quantity of titanium atom left in the surface. Furthermore, the shift in the Ti 2p binding energy is a result of the titanium atom in different chemical environment and yields a slightly different XPS peaks. The presence of the molecular oxygen in the air-side is a probable explanation for why the surface titanium atom has higher binding energy, while the titanium atom in the bulk has lower binding energy. Due to the lack of molecular oxygen in the bulk, the transition from $Ti(OEt)_4$ to titanium oxide is not complete. Thus, there may be existed many kinds of titanium compounds such as Ti–C, Ti–O, etc. Conversely, it can be said that the much amount of oxygen in the air-side, the conversion of $Ti(OEt)_4$ to titanium dioxide is more extensively compared to the bulk one. Fig. 7 shows the intensity of Ti 2p increases with increasing the amounts of TiO_2. Here, the shift in the Ti 2p binding energy is according to the same reason described as above. Because of the more titanium atoms exist in the hybrid film, the more complex compounds will be formed such as Ti–Ti, Ti–O–Ti, etc. XPS reveals quantitative information of surface composition ($\leq$50 Å) of the hybrid films. The molar percent is calculated under an assumption that all the titanium alkoxide converted to TiO_2. Table 1 lists the surface content of Ti in the hybrid films by XPS measurements. As seen from Table 1, a molar percentage of experimental values are much less than the theoretical bulk Ti content. In addition, the ratio of experiment value to

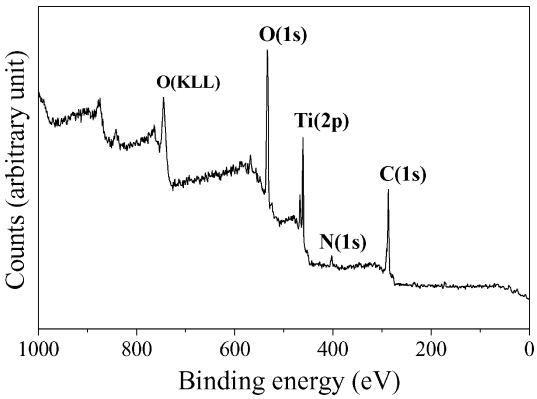

Fig. 5. XPS survey spectrum of the PI/TiO_2-40 wt% hybrid film.

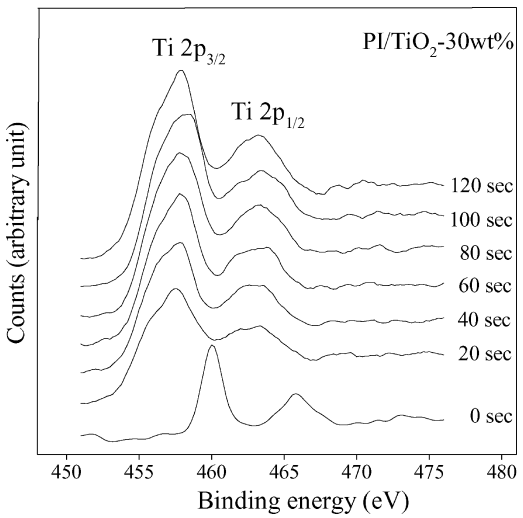

Fig. 6. Ti 2p region of XPS spectra recorded at different sputtering times of PI/TiO_2-30 wt% hybrid film.

theoretical one increases with the Ti content as TiO_2 wt% < 20 and the ratio reaches a constant as TiO_2 wt% ≥ 20. Apparently, the surface concentration of TiO_2 is lower than that in the bulk. The result is consistent with the statement of Fig. 6.

Fig. 8(a) and (b) show the cross-sectional TEM images of PI/TiO_2-5 wt% and PI/TiO_2-30 wt%, respectively. The particle sizes of TiO_2 in PI/TiO_2-5 wt% and PI/TiO_2-30 wt% are 10 and 40 nm. This indicates that the particle size increases with the increasing TiO_2 content. TEM reveals a uniform dispersion of spherical shaped particles throughout the PI/TiO_2 hybrid films. The spatial distribution of PI/TiO_2-30 wt% is denser than PI/TiO_2-5 wt%. Moreover, the high glass-transition temperature of polyimide would be expected to further stabilize the nanoparticles by decreasing their mobility, thereby preventing TiO_2 agglomeration into large particles. Fig. 9(a) and (b) are the selected-area electron diffraction (SAED) pattern of the dark area in Fig. 8. Both of them indicate the same diffraction facets of

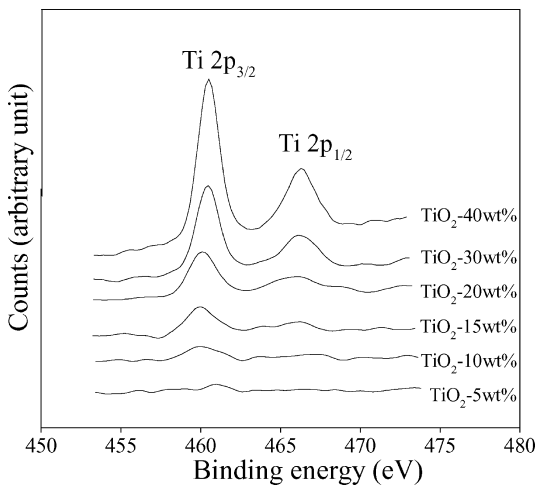

Fig. 7. XPS spectra of Ti 2p in hybrid films.

Table 1
The surface content of TiO_2 in PI/TiO_2 hybrid films by XPS measurements

Sample	Experimental value Ti (mol%)	Theoretical value Ti (mol%)	Experimental value/theoretical value
PI/TiO_2-5 wt%	0.13	0.86	0.15
PI/TiO_2-10 wt%	0.53	1.80	0.29
PI/TiO_2-15 wt%	0.92	2.83	0.33
PI/TiO_2-20 wt%	1.38	3.95	0.35
PI/TiO_2-30 wt%	3.17	6.60	0.34
PI/TiO_2-40 wt%	3.37	9.90	0.34

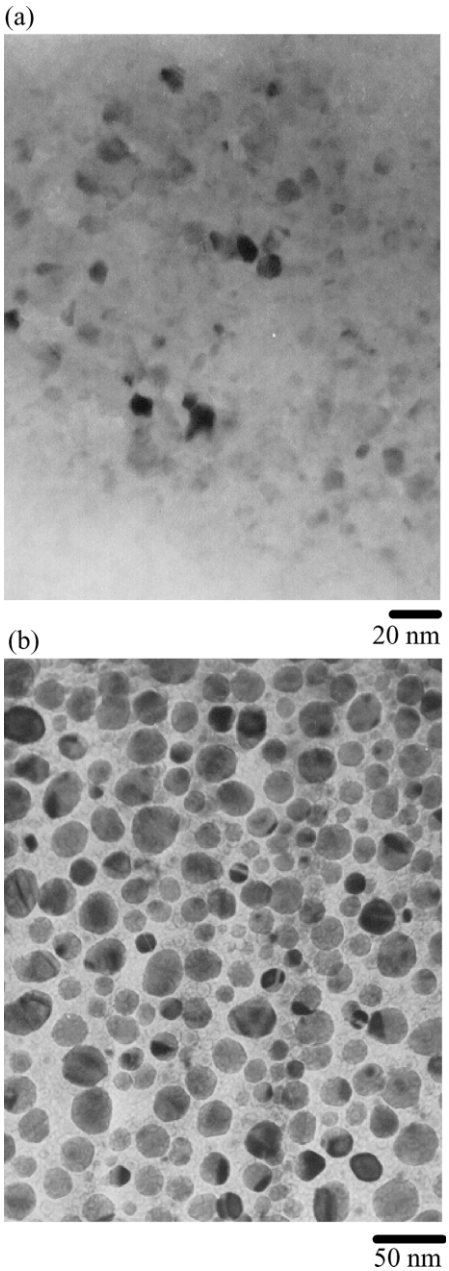

Fig. 8. TEM photographs of the hybrid films (a) PI/TiO_2-5 wt% (b) PI/TiO_2-30 wt%.

the TiO2 phase, meaning (200), (112), (040), (400) and (351), respectively.

The thermal gravimetric profiles of the PI/TiO_2 nanocomposite films are shown in Fig. 10. The introduction of TiO_2 causes only a slight decrease (40 °C) in thermal stability of hybrid films compared to the pure PI when tested in nitrogen. Boggess and Taylor have pointed out that metallic compounds can oxidatively degrade polyimide films [34]. The dramatic decrease in thermal stability of hybrid films can probably be attributed to metal-catalyzed oxidative decomposition pathways in the composite [11,35].

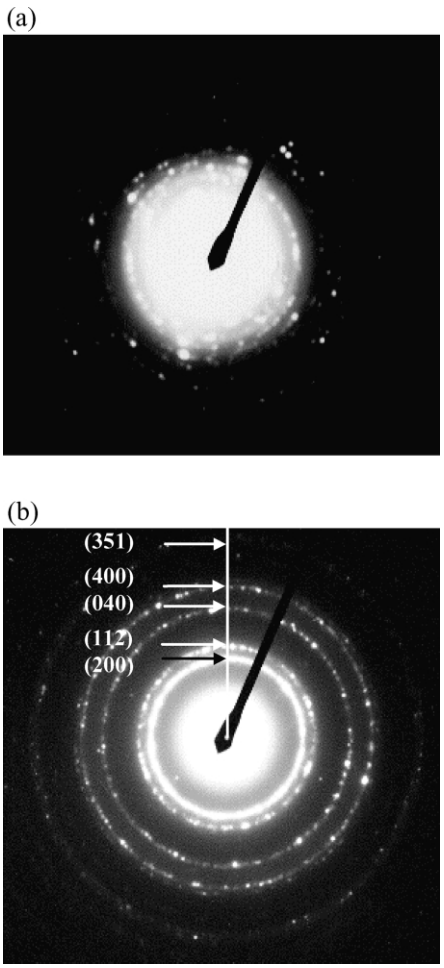

Fig. 9. Selected-area electron diffraction (SAED) patterns (a) PI/TiO_2-5 wt% (b) PI/TiO_2-30 wt%.

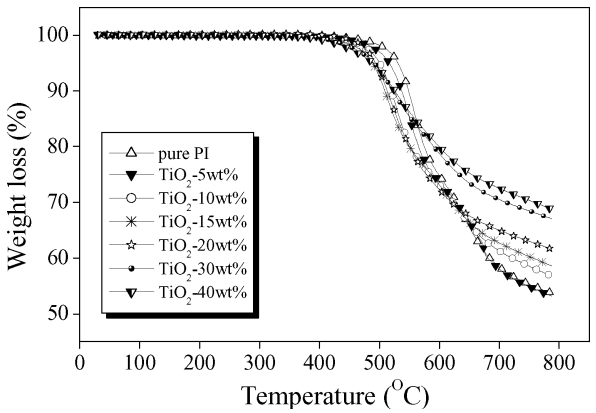

Fig. 10. Thermogravimetric profiles of the PI/TiO_2 hybrid films.

Although the thermal stability of the hybrid films is inferior to pure PI, it is still pretty good for the practical application.

4. Conclusion

PI/TiO_2 hybrid films of BAO/ODPA polyimide containing TiO_2 nanocrystallite have been prepared by the sol–gel method. The new PI/TiO_2 hybrid films have fair good optical transparency, even with TiO_2 content up to 40 wt%. The TiO_2 nanocrystallines is well dispersed in the PI matrix with 10–40 nm in diameter when the TiO_2 content is from 5 to 30 wt%. The surface TiO_2 content increases with the bulk TiO_2 content in all compositions. However, the ratio of the surface TiO_2 to the bulk TiO_2 increases with the TiO_2 content as it <20 wt%, and levels off as the TiO_2 content ≥ 20 wt%. The shift in the titanium signal of XPS spectra is may be related to the titanium atom in different chemical states when the titanium alkoxide converted to titanium oxide. The binding energy shifts cover a change of about 2 eV. The SAED pattern is observed. The SAED diffraction pattern shows the facets of TiO_2 crystalline (200), (112), (040), (400) and (351), respectively. Moreover, the hybrid films still possess good thermal stability.

Acknowledgements

The authors would like to acknowledge the financial support of the National Science Council through project NSC 91-2216-E-009-013, Taimide Technology Company and Lee and MTI Center for Networking Research.

References

[1] Wen J, Wilkes GL. Chem. Mater. 1996;8:1667.
[2] Mark JE. Polym. Eng. Sci. 1996;36:2905.
[3] Hide F, Nito K, Yasuda A. Thin Solid Film 1994;240:157.
[4] Ahmad Z, Sarwar MI, Wang S, Mark JE. Polymer 1997;38(17):4523.
[5] Cornelius CJ, Marand E. Polymer 2002;43:2385.
[6] Delozier DM, Orwoll RA, Cahoon JF, Johnston NJ, Smith JG, Connell JW. Polymer 2002;43:813.
[7] Sroog CE. J Polym Sci Macromol Rev 1976;11:161.
[8] Mittal KL, editor. Polyimide: synthesis, characyerization and application. New York: Plenum Press; 1984.
[9] Ghosh MK, Mittal KL, editors. Polyimide, fundamentals and applications. New York: Marcel Dekker; 1996.
[10] Angelo RJ. US Patent 1959, 3, 073,785.
[11] Sawada T, Ando S. Chem Mater 1998;10:3368.
[12] Clair A, NASA-Langley Research Center, Taylor LT. J Appl Polym Sci 1983;28:2393.
[13] Ellison MM, Taylor LT. Chem Mater 1994;6:990.
[14] Rancourt JD, Porta GM, Taylor LT. Thin Solid Films 1988;158:189.
[15] Zeng W, Qiu W, Liu J, Yang X, Lu L, Wang X. Polymer 1995;36(19):3761.
[16] Chang CC, Chen WC. J Polym Sci, Part A: Polym Chem 2001;39:3419.
[17] Tong YJ, Li YS, Xie FC, Ding MX. Polym Int 2000;49:1543.
[18] Yoshida M, Lal M, Kumar ND, Prasad PN. J Mater Sci 1997;32:4047.
[19] Yoshida M, Paras NP. Chem Mater 1996;8:235.
[20] Que W, Zhou Y, Lam YL, Chan YC, Kam CH. Thin Solid Films 2000;358:16.
[21] Tyan HL, Liu YC, Wei KH. Polymer 1999;40:4877.
[22] Liu L, Lu Q, Yin J, Qian X, Wang W, Zhu Z, Wang Z. Mater Chem Phys 2002;74:210.
[23] Hu Q, Marand E. Polymer 1999;40:4833.
[24] Lee LH, Chen WC. Chem Mater 2001;13:1137.
[25] Zhang J, Wang BJ, Ju X, Liu T, Hu TD. Polymer 2001;42:3697.
[26] Heberer DP, Cheng SZD, Barley JS, Lien SHS, Bryant RG, Harris FW. Macromolecules 1991;24(8):1890.
[27] Rogers ME, Brink MH, Mcgrath JE, Brennan A. Polymer 1993;34(4):849.
[28] Koning C, Teuwen L, Meijer EW, Moonen J. Polymer 1994;35(22):4889.
[29] Liu XQ, Yamanaka K, Jikei M. Chem Mater 2000;12(12):3885.
[30] Tamai S, Kuroki T, Shibuya A. Polymer 2001;42(6):2373.
[31] Benjaram MR, Biswajit C. Langmuir 2001;17:1132.
[32] Bedri E, Robert AH, Gary WS, David S, Victoria LD, Mohamed S. Langmuir 2001;17:2664.
[33] Christophe G, Evelyne D, Philippe D, Michel D. J Electron Spectrosc Related Phenom 1994;70:11.
[34] Boggess RK, Taylor LT. J Polym Sci, Polym Chem Ed 1987;25:685.
[35] Rancourt JD, Taylor LT. Macromolecules 1987;20:790.
[36] Wang B, Wilkes GL, Hedrick JC, Liptak SC, McGrath JE. Macromolecules 1991;24:3449.
[37] Papadimitrakopoulos P, Wisniecki P, Bhagwagar D. Chem Mater 1997;9:2928.
[38] Lee LH, Chen WC. Chem Mater 2001;13:1137.
[39] Sanchez C, Livage J, Henry M, Babonneau F. J Non-Cryst Solid 1988;100:65.